

Phase transitions of a single polyelectrolyte in a poor solvent with explicit counterions

Anoop Varghese,* Satyavani Vemparala,† and R. Rajesh‡

The Institute of Mathematical Sciences, C.I.T. Campus, Taramani, Chennai 600113, India

(Dated: September 30, 2010)

Conformational properties of a single flexible polyelectrolyte chain in a poor solvent are studied using constant temperature molecular dynamics simulation. The effects of counterions are explicitly taken in to account. Structural properties of various phases and the transition between these phases are studied by tracking the values of asphericity, radius of gyration, fraction of condensed counterions, number of non-bonded neighbours and Coulomb interaction energies. From our simulations, we find strong evidence for a first-order phase transition from extended to collapsed phase consistent with earlier theoretical predictions. We also identify a continuous phase transition associated with Manning condensation of counter ions and estimate the critical exponents associated with such transition. Finally, we argue that previous suggestions of existence of an independent intermediate phase between extended and collapsed phases is only a finite size effect.

PACS numbers: 82.35.Rs,36.20.Ey,64.70.km

I. INTRODUCTION

Polyelectrolytes are polymers, which in a polar solvent, release counterions into the solution, making the polymer backbone charged. Examples of polyelectrolytes include sulfonated polystyrene, polymethacrylic acid, DNA, RNA and proteins. Though the system is overall charge neutral, long range Coulomb interactions make the behaviour of polyelectrolytes considerably different from that of neutral polymers [1, 2]. The static and dynamic properties of polyelectrolytes depend on the nature of the solvent, linear charge density of the polymer backbone, valency of the counterions, temperature, salt concentration, hydrodynamic interactions and the bending rigidity [1, 3].

A polyelectrolyte chain in a poor solvent undergoes a series of phase transitions as the linear charge density of the chain is varied keeping temperature fixed. The rich phase diagram resulting from a competition between the long range Coulomb interaction and the short range excluded volume interaction has been studied theoretically [4–9], numerically [6, 10–14] and experimentally [15–20]. At very low charge densities, the polyelectrolyte chain is in a collapsed phase, with the counterions uniformly distributed throughout the solution [14]. On increasing the charge density, the polyelectrolyte chain makes a transition into the pearl-necklace phase in which the chain has two (dumbbell) or more globules connected through a string of monomers [4, 5, 7]. This instability of the charged collapsed phase is similar to the Rayleigh instability of a charged droplet [21]. While the pearl-necklace phase has been observed in numerical simulations [13, 14, 22], the experimental status is unclear [15]. Further increase in charge density decreases the number

and size of the globules and the polyelectrolyte chain becomes extended. When the linear charge density exceeds a threshold value, the electrostatic energy dominates over the thermal fluctuations and the counterions condense on the polyelectrolyte chain [8]. The condensed counterions form dipoles with the polymer monomers and the attraction among the dipoles leads to the collapse of the polyelectrolyte chain [11]. Recent simulations also show that, in extreme poor solvent conditions, the polyelectrolyte chain can make a direct transition from the initial collapsed phase to the final condensed collapsed phase without encountering some or even all the intermediate phases [14].

Certain features of the phase diagram remain poorly understood. Recent simulations argue for the existence of an intermediate phase between the extended and the condensed collapsed phases [13, 14]. Referred to as the sausage phase, this phase is defined as a collapsed phase in which the shape of the collapsed polymer becomes aspherical, having a non-zero mean asphericity. It is not clear whether this phase is just a finite size effect.

In addition the nature of the Manning condensation of counterions is not well understood. By studying analytically the condensation of counterions on a disc in two dimensions, it was shown that condensation is a second order phase transition [23–25]. However, to the best of our knowledge, the corresponding question has not been answered for a polyelectrolyte chain.

In this paper we simulate polyelectrolyte chains of different lengths and varying charge densities. We argue that the sausage phase does not exist and is an artefact of studying very small chains. Our simulations also show strong evidence that the counterion condensation is a second order transition accompanied by a divergence in the fluctuations of the number of non-bonded nearest neighbours of a monomer. In addition, we study aspects of the condensed collapsed transition.

*anoop@imsc.res.in

†vani@imsc.res.in

‡rrajesh@imsc.res.in

II. MODEL AND SIMULATION METHOD

We model the polyelectrolyte chain as spherical beads (monomers) connected through springs where each monomer carries a charge qe . Counterions are modelled as spherical beads, each carrying a charge $-qe$. The polyelectrolyte chain and the counterions are assumed to be in a medium of uniform dielectric constant ϵ . The potential energy due to the pair of particles i and j consists of three interactions.

Coulomb interaction: The electrostatic energy is given by

$$U_c(r_{ij}) = \frac{Zq^2e^2}{4\pi\epsilon r_{ij}}, \quad (1)$$

where $Z = -1$ for monomer-counterion pairs and $Z = 1$ otherwise, and r_{ij} is the distance between particle i and j . For computational efficiency, $U_c(r_{ij})$ is set to zero beyond a cut off distance. The cut off distance is chosen to be order of the system size so that the long range nature of the Coulomb interaction is maintained.

Excluded volume interaction: The excluded volume interactions are modelled by the Lennard-Jones potential, which for two particles at a distance r_{ij} , is given by

$$U_{LJ}(r_{ij}) = 4\epsilon_{ij} \left[\left(\frac{\sigma}{r_{ij}} \right)^{12} - \left(\frac{\sigma}{r_{ij}} \right)^6 \right], \quad (2)$$

where ϵ_{ij} is the minimum of the potential and σ is the inter particle distance at which the potential becomes zero. We set the depth of the attractive potential ϵ_{ij} as 1.0 for monomer-counterion and counterion-counterion pairs and 2.0 for monomer pairs, while σ is set to 1.0 for all pairs. We use the shifted Lennard-Jones potential in which $U_{LJ}(r_{ij})$ is set to zero beyond a cut off distance r_c . The value of r_c equals σ for monomer-counterion and counterion-counterion pairs and 2.5σ for monomer-monomer pairs. With this choice of the parameters, the excluded volume interaction is purely repulsive for all the pairs other than the monomer-monomer pairs. The effective short range attraction among the monomers mimics poor solvent conditions. Other ways of realising poor solvent conditions may be found in Ref. [22].

Bond stretching interaction: The bond stretching energy for pairs in the polymer that are connected directly through springs is given by

$$U_{bond}(r_{ij}) = \frac{1}{2}k(r_{ij} - b)^2, \quad (3)$$

where k is the spring constant and b is the equilibrium bond length. The values of k and b are taken as 500 and 1.12 respectively. This value of b is close to the minimum of Lennard-Jones potential.

The relative strength of the electrostatic interaction is parametrised by a dimensionless quantity A :

$$A = \frac{q^2\ell_B}{b}, \quad (4)$$

where ℓ_B is the Bjerrum length [26], the length scale below which electrostatic interaction dominates thermal fluctuations.

$$\ell_B = \frac{e^2}{4\pi\epsilon_0\epsilon k_B T}, \quad (5)$$

where k_B is the Boltzmann constant and T is temperature. The thermal fluctuations dominate over the electrostatic interactions for very low values of A and the counterions will be uniformly distributed in the solution. When A is of order one, the electrostatic interaction energy is comparable to the thermal energy and the counterions begin to undergo Manning condensation[8].

The time integration of the equations of motion is done using the molecular dynamics simulation package LAMMPS [27, 28]. The simulations are done at constant temperature ($T=1.0$), maintained through a Nose-Hoover thermostat [29, 30]. The size of the simulation box is 1.2 times the length of the extended chain. Periodic boundary conditions are used. The initial configuration of the chain is a randomly chosen one while the counterions are distributed uniformly throughout the volume. All the averages are calculated over 10^5 configurations after the system is equilibrated.

III. RESULTS AND DISCUSSION

A. Configurations of the polyelectrolyte chain

Snap shots of the polyelectrolyte configurations for different values of A are shown in Fig. 1. For very small values of A , the electrostatic interactions can be ignored, and the polymer exists in a collapsed phase [Fig. 1(a)]. As A is increased, the globule breaks up into two [Fig. 1(b)] or more smaller globules [Fig. 1(c)]. This pearl-necklace configuration becomes extended on further increasing A [Fig. 1(d)]. Counterion condensation is initiated and for sufficiently large A , the polymer undergoes a collapse transition to form a sausage phase [14] [Fig. 1(e)] or a spherical globule [Fig. 1(f)].

B. Distribution of counterions

We consider a counterion to be condensed if its distance from any one monomer is less than $2\ell_B$. Let N_c be the number of condensed counterions and N the number of monomers. The mean fraction of condensed counterions $\langle N_c/N \rangle$ as a function of A is shown in Fig. 2 for different N . The counterion condensation starts before the Manning threshold value ($A = 1$) is reached, consistent with the findings in Ref. [31]. For fixed value of A , the fraction $\langle N_c/N \rangle$ decreases with N for $A \lesssim 6.0$, which corresponds to the entire extended phase (see Sec. III D). This is in contrast with the behaviour of a polyelectrolyte chain in a good solvent where it has been observed [11] that, for fixed A , the fraction of condensed counterions

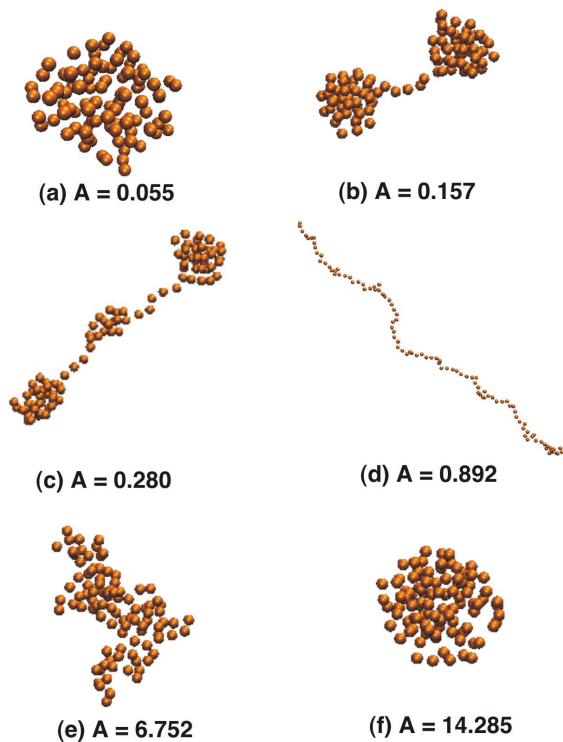


FIG. 1. Snapshots of the polyelectrolyte chain configurations for different values of A . For the sake of clarity, counterions are not shown and figures are not in the same scale. (a) Globular phase, (b) Dumbbell phase, (c) Pearl-necklace phase, (d) Extended phase, (e) Sausage phase and (f) Globular phase.

increases with N for all A in the extended phase. Below, we argue that this is so because for the same A , longer chains are relatively more extended than shorter chains.

We first note that the fraction of condensed counterions depends on the chain morphology. The chain morphology can be varied by tuning the monomer-monomer attractive interaction parameter ϵ_{mm} keeping other parameters the same. The fraction of condensed counterions increases with increasing ϵ_{mm} (see inset of Fig. 2). It is clear that increasing ϵ_{mm} can only result in the size of the polyelectrolyte chain becoming smaller. A smaller size implies that the counterions can experience lower electrostatic potential, and hence condense more when ϵ_{mm} is increased.

We now show that longer chains have a larger effective size in the extended phase ($A \lesssim 6.0$). To study the size dependence on N , we calculate the radius of gyration R_g , defined as

$$R_g = \sqrt{\frac{1}{N} \sum_{i=1}^N (\vec{r}_i - \vec{r}_{cm})^2}, \quad (6)$$

where \vec{r}_i is the position of the i^{th} particle and \vec{r}_{cm} is the centre of mass of the chain. For fixed A , R_g/N , a measure of the relative extension, increases with N in the extended phase (see Fig. 3). Thus, the effective size

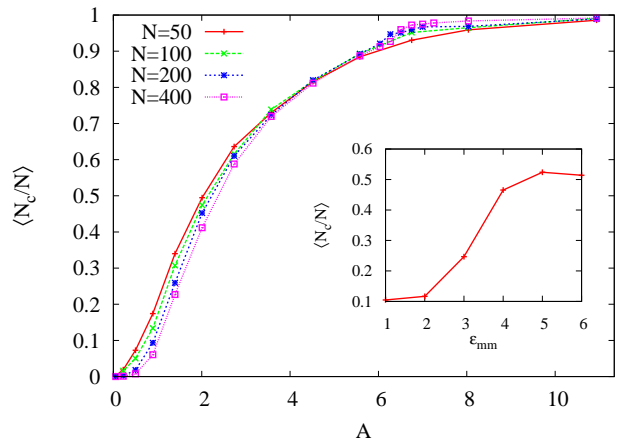


FIG. 2. Mean fraction of counterions $\langle N_c/N \rangle$ within a distance $2\ell_B$ from the polyelectrolyte chain as a function of A . Inset: $\langle N_c/N \rangle$ as a function of the monomer-monomer attraction energy ϵ_{mm} for $N = 100$ and $A = 0.89$.

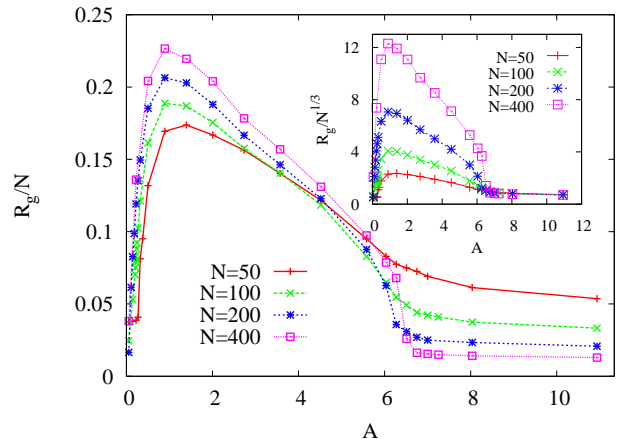


FIG. 3. Ratio of the radius of gyration R_g to the number of monomers N as a function of A . Inset: The data for $R_g/N^{1/3}$ collapse for different N for $A \gtrsim 6.25$.

is larger for larger chains, and hence smaller chains have a larger fraction of condensed counterions.

C. Number of non-bonded neighbours and the condensation transition

The number of non-bonded nearest neighbours of a monomer is a useful order parameter in studying the collapse transition of a neutral polymer [32]. We study its behaviour for the polyelectrolyte chain. A monomer or counterion is defined to be a non-bonded neighbour of a given monomer if its distance from it is less than b , not connected to it by a bond. The variation of the mean number of non bonded neighbours per monomer $\langle n_b \rangle$ with A is shown in Fig. 4. $\langle n_b \rangle$ decreases when the poly-

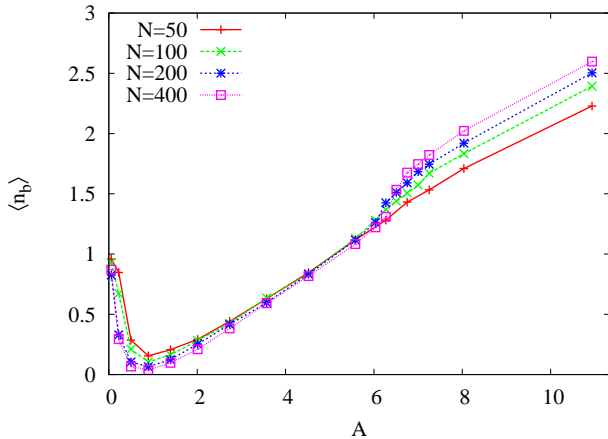


FIG. 4. The number of non bonded neighbours per monomer $\langle n_b \rangle$ as a function of A for different N

electrolyte chain goes from the initial collapsed phase to the extended phase. It has the minimum around $A \sim 1.0$ where the chain is most extended. Close to $A_c \approx 6.25$, $\langle n_b \rangle$ has a jump with the jump size increasing with number of monomers N . This value of A corresponds to the collapse transition of the condensed polyelectrolyte (see inset of Fig. 3).

We also study the relative fluctuations χ_b of the number of non-bonded neighbours, where

$$\chi_b = \frac{N [\langle n_b^2 \rangle - \langle n_b \rangle^2]}{\langle n_b \rangle^2}. \quad (7)$$

It has a peak at $A' \approx 0.89$ (see Fig. 5). The peak height increases with number of monomers N , showing a divergence in the thermodynamic limit. This critical value of A corresponds to the onset of Manning condensation of the counterions. The data for different N 's can be collapsed using the scaling form

$$\chi_b \approx N^{\phi_1} f[(A - A')N^{\phi_2}], \quad N \gg 1, \quad (8)$$

where ϕ_1 and ϕ_2 are exponents. Data collapse is seen for $\phi_1 \approx 0.7$ and $\phi_2 \approx 0.3$ (see inset of Fig. 5). Divergence of χ_b with data collapse is a strong indication of condensation being a continuous phase transition. Earlier discussion of the order of the Manning condensation has been restricted only to model systems of discs in two dimensions. A similar continuous transition has been predicted in such systems [23–25].

D. Transition from extended phase to collapsed phase

To quantify the transition from the extended phase to the collapsed phase, the electrostatic energy per monomer E_c and its fluctuations are calculated. Only monomer–monomer pairs are used for calculating these

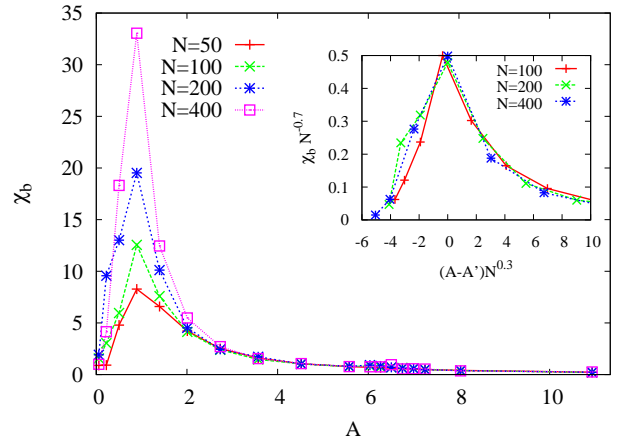


FIG. 5. The relative fluctuation χ_b of the number of non bonded neighbours, as defined in Eq. (7), as a function of A for different N . Inset: Data collapse when χ_b and A are scaled as in Eq. (8)

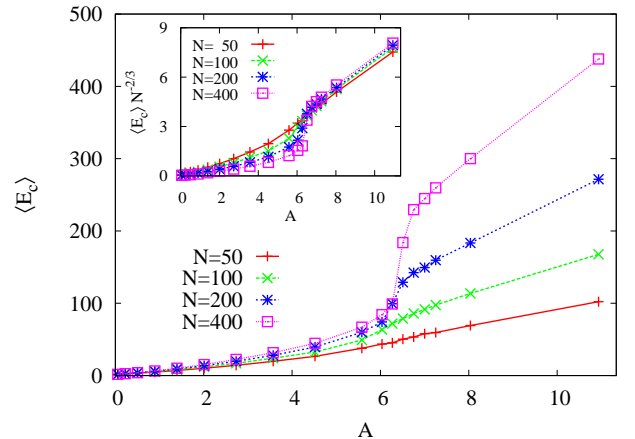


FIG. 6. Mean Coulomb energy per monomer $\langle E_c \rangle$ as a function of A for different N . Inset: $\langle E_c \rangle \sim N^{2/3}$ in the collapsed phase.

quantities since we are interested in the configuration of the polyelectrolyte chain. The relative fluctuation χ_c in the electrostatic energy is defined as

$$\chi_c = \frac{N [\langle E_c^2 \rangle - \langle E_c \rangle^2]}{\langle E_c \rangle^2}. \quad (9)$$

The mean electrostatic energy per monomer $\langle E_c \rangle$ increases with A and has an abrupt jump at $A_c \approx 6.25$ (see Fig. 6). The jump is more pronounced for higher values of N . In the collapsed phase, the shape of the chain is roughly spherical and hence $\langle E_c \rangle$ should scale as $N^{2/3}$ [33]. For $A > A_c$, $\langle E_c \rangle$ does scale as $N^{2/3}$ (see inset of Fig. 6). We show that the polymer is indeed in the collapsed phase by confirming that the radius of gyration R_g is proportional to $N^{1/3}$ (see inset of Fig. 3).

The variation of the relative fluctuation χ_c with A is

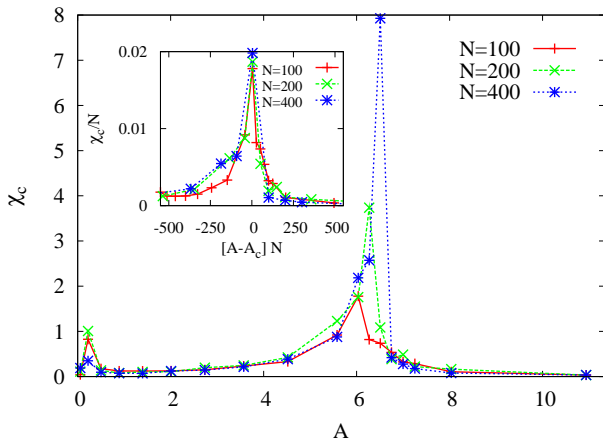


FIG. 7. Fluctuation in the Coulomb energy per monomer χ_c as a function of A . Inset: Data collapse when χ_c and A are scaled as in Eq. (8).

shown in Fig. 7. χ_c has a peak at A_c , close to the value of A at which $\langle E_c \rangle$ has a discontinuity. The height of the peak increases with the number of monomers, diverging in the thermodynamic limit. The collapse transition is expected to be first order [34] and the jump in $\langle E_c \rangle / N^{2/3}$ is consistent with it. For a first order transition, χ_c should have the scaling form [35]

$$\chi_c \approx N f[(A - A_c)N], \quad N \gg 1, \quad (10)$$

Reasonable data collapse is obtained when χ_c and A are scaled as in Eq. (10) [see inset of Fig. 7].

E. Existence of Sausage phase

The sausage phase was defined in Ref. [14] as a collapsed phase where mean asphericity is non-zero. We do an analysis of asphericity and show that the transition associated with change in asphericity coincides with the collapse transition. We define asphericity Y as

$$Y = \left\langle \frac{\lambda_1 - \frac{\lambda_2 + \lambda_3}{2}}{\lambda_1 + \lambda_2 + \lambda_3} \right\rangle, \quad (11)$$

where $\lambda_{1,2,3}$ are the eigenvalues of the moment of inertia tensor with λ_1 being the largest eigenvalue. The moment of inertia tensor G is

$$G_{\alpha\beta} = \frac{1}{N} \sum_{i=1}^N r_{i\alpha} r_{i\beta}, \quad (12)$$

where $r_{i\alpha}$ is the α^{th} component of the position vector \vec{r}_i . Asphericity Y is zero for a sphere (collapsed globule) and one for a linear rod (extended configuration). For all other configurations, it has a value between zero and one.

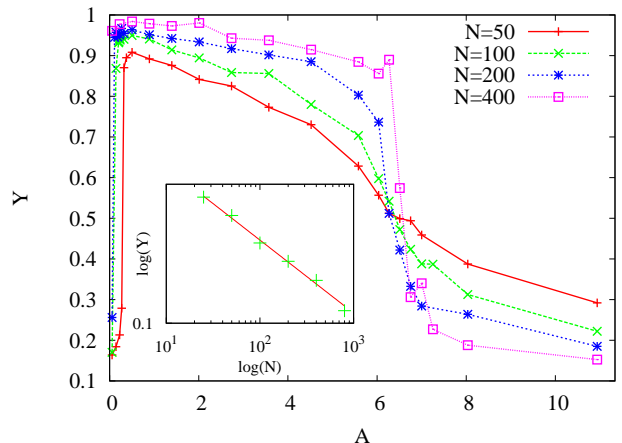


FIG. 8. Asphericity Y (as defined in Eq. (11)) as a function of A . Inset: Variation of Y with N for $A = 10.93$. The slope of the straight line is -0.3 .

The variation of asphericity with A for different N is shown in Fig. 8. For very small values of A , asphericity increases corresponding to the extension of the initial collapsed phase. In the extended region $A \lesssim 6.25$, asphericity increases with N and tends to one when $N \rightarrow \infty$. For $A \gtrsim 6.25$, asphericity decreases with N and tends to zero as a power law when $N \rightarrow \infty$ (see inset of Fig. 8). Thus, in the thermodynamic limit, asphericity jumps from one to zero as A crosses $A_c \approx 6.25$. This transition coincides with extended to collapsed transition discussed in Sec. III D. As there is no second transition in asphericity or in χ_c , we conclude that the sausage phase suggested in Ref. [14] is identical with the collapsed phase and is not a different phase.

IV. CONCLUSIONS

Using molecular dynamics simulations, we studied the phase diagram and phase transitions between the phases of a single polyelectrolyte chain in a poor solvent. The counterions were taken care of explicitly while the solvent was implicit. The dependence of various physical quantities on A , a dimensionless number that parametrised the strength of the electrostatic interaction, were calculated for different chain lengths N . Our main results are summarised below.

We quantified the transition associated with the Manning condensation of counterions on the extended chain. The fluctuations of the non-bonded neighbours χ_b diverges at $A \approx 0.89$ with exponents that indicate a continuous transition. While the value of the exponents we obtained are not accurate, they indicate that data for different system sizes can be explained by one scaling function. It would be interesting to study the number of non-bonded neighbours and its fluctuations for the good solvent problem as well as in the presence of salt.

We also analysed the sausage phase introduced in Ref. [14] as a new intermediate phase between the extended and collapsed phases. We show that the transition associated with the discontinuity in asphericity and that associated with the extended to collapsed transition occur, within numerical error, at the same value of A ($A \approx 6.25$). This, in conjunction with the fact that there is no second transition for either quantity, strongly suggest that the sausage phase does not exist independent of the collapsed phase, and was probably an artefact of earlier simulations [14] being for chains of small size.

The extended to collapsed transition of the condensed polymer chain was also quantified. The abrupt jump

in $R_g/N^{1/3}$, in the mean electrostatic energy $\langle E_c \rangle$, and mean number of non-bonded nearest neighbours $\langle n_b \rangle$, combined with the fluctuations of the electrostatic energy χ_c having a peak proportional to N , is strong evidence for a first order transition. This is consistent with the theoretical prediction in [34].

In addition, we find that the fraction of condensed counterions decreases with N for fixed A in the extended phase. By studying its dependence on ϵ_{mm} and the dependence of R_g/N on N , we argued that the decrease in the fraction is related to longer chains having a larger relative extension.

-
- [1] A. V. Dobrynin and M. Rubinstein, *Prog. Polym. Sci* **30**, 1049 (2005).
- [2] Y. Levin, *Rep. Prog. Phys.* **65**, 1577 (2002).
- [3] R. R. Netz and D. Andelman, "Encyclopedia of electrochemistry," (Wiley-VCH, 2002) p. 282.
- [4] Y. Kantor and M. Kardar, *Europhys. Lett* **27**, 643 (1994).
- [5] Y. Kantor and M. Kardar, *Phys. Rev. E* **51**, 1299 (1995).
- [6] Q. Liao, A. V. Dobrynin, and M. Rubinstein, *Macromolecules* **39**, 1920 (2006).
- [7] A. V. Dobrynin, M. Rubinstein, and S. P. Obukhov, *Macromolecules* **29**, 2974 (1996).
- [8] G. S. Manning, *J. Chem. Phys* **51**, 924 (1969).
- [9] M. Muthukumar, *J. Chem. Phys* **120**, 9343 (2004).
- [10] H. Schiessel and P. Pincus, *Macromolecules* **31**, 7953 (1998).
- [11] R. Winkler, M. Gold, and P. Reineker, *Phys. Rev. Lett* **80**, 3731 (1998).
- [12] P. Loh, G. R. Deen, D. Vollmer, K. Fischer, M. Schmidt, A. Kundagrami, and M. Muthukumar, *Macromolecules* **41**, 9352 (2008).
- [13] H. J. Limbach and C. Holm, *J. Phys. Chem. B* **107**, 8041 (2003).
- [14] K. Jayasree, P. Ranjith, M. Rao, and P. B. S. Kumar, *J. Chem. Phys* **130**, 094901 (2009).
- [15] V. O. Aseyev, S. I. Klenin, H. Tenhu, I. Grillo, and E. Geissler, *Macromolecules* **34**, 3706 (2001).
- [16] C. E. Williams and M. D. C. Tinoco, *Europhys. Lett* **52**, 284 (2000).
- [17] M. D. C. Tinoco, R. Ober, I. Dolbnya, W. Bras, and C. E. Williams, *J. Phys. Chem. B* **106**, 12165 (2002).
- [18] M. N. Spiteri, C. E. Williams, and F. Boue, *Macromolecules* **40**, 6679 (2007).
- [19] V. O. Aseyev, H. Tenhu, and S. I. Klenin, *Macromolecules* **32**, 1838 (1999).
- [20] F. Bordini, C. Cametti, T. Gili, S. Sennato, S. D. S. Zuzzi, and R. H. Colby, *Phys. Rev. E* **72**, 031806 (2005).
- [21] L. Rayleigh, *Phil. Mag* **14**, 184 (1882).
- [22] R. Chang and A. Yethiraj, *J. Chem. Phys* **118**, 14 (2003).
- [23] A. Naji and R. R. Netz, *Phys. Rev. Lett.* **95**, 185703 (2005).
- [24] A. Naji and R. R. Netz, *Phys. Rev. E* **73**, 056105 (2006).
- [25] Y. Burak and H. Orland, *Phys. Rev. E* **73**, 010501(R) (2006).
- [26] W. B. Russel, D. A. Saville, and W. R. Schowalter, *Colloidal Dispersions* (Cambridge University Press, Cambridge, 1989).
- [27] <http://lammmps.sandia.gov>.
- [28] S. J. Plimpton, *J. Comp. Phys* **117**, 1 (1995).
- [29] S. Nose, *J. Chem. Phys* **51**, 511 (1984).
- [30] W. G. Hoover, *Phys. Rev. A* **31**, 1695 (1985).
- [31] S. Liu and M. Muthukumar, *J. Chem. Phys.* **116**, 9975 (2002).
- [32] C. Vanderzande, *Lattice Models of Polymers* (Cambridge University Press, Cambridge, 1999).
- [33] L. D. Landau and E. M. Lifshitz, *Classical Theory of Fields* (Butterworth-Heinemann, Oxford, 1975).
- [34] N. V. Brilliantov, D. V. Kuznetsov, and R. Klein, *Phys. Rev. Lett* **81**, 1433 (1998).
- [35] K. Binder, *Rep. Prog. Phys.* **60**, 487 (1997).